NIH Public Access
Author Manuscript
Auton Neurosci. Author manuscript; available in PMC 2008 October 30.

Published in final edited form as:
Auton Neurosci. 2007 October 30; 136(1-2): 31–42.

Ultrastructural Evidence for Selective Noradrenergic Innervation of CNS Vagal Projections to the Fundus of the Rat

Rebecca J. Pearson[1], **Philip J. Gatti**[2], **Niaz Sahibzada**[1], **V. John Massari**[2], and **Richard A. Gillis**[1]

1 *Department of Pharmacology, Georgetown University Medical Center, Washington, DC*

2 *Department of Pharmacology, Howard University Medical Center, Washington, DC*

Abstract

We reported pharmacological data suggesting that stimulation of the vago-vagal reflex activates noradrenergic neurons in the hindbrain that inhibit dorsal motor nucleus of the vagus (DMV) neurons projecting to the fundus, but not to the antrum (Ferreira et al., 2002). The purpose of this study was to use an ultrastructural approach to test the hypothesis that noradrenergic terminals form synapses with DMV fundus-projecting neurons, but not with DMV antrum-projecting neurons. A retrograde tracer, CTβ-HRP, was injected into the gastric smooth muscle of either the fundus or the antrum of rats. Animals were re-anesthetized 48 hours later and perfusion-fixed with acrolein and paraformaldehyde. Brainstems were processed histochemically for CTβ-HRP, and immunocytochemically for either DβH or PNMT by dual-labeling electron microscopic methods. Most cell bodies and dendrites of neurons that were retrogradely labeled from the stomach occurred at the level of the area postrema. Examination of 482 synapses on 238 neurons that projected to the fundus revealed that 17.4 +/− 2.7% (n=4) of synaptic contacts were with DβH-IR terminals. Of 165 fundus-projecting neurons, 4.4 +/− 1.5 % (n=4) formed synaptic contacts with PNMT-IR terminals. In contrast, the examination of 384 synapses on 223 antrum-projecting neurons revealed no synaptic contact with DβH-IR terminals. These data provide proof that norepinephrine containing nerve terminals synapse with DMV fundus projecting neurons but not with DMV antrum-projecting neurons. These data also suggest that brainstem circuitry controlling the fundus differs from circuitry controlling the antrum.

3. INTRODUCTION

Based on smooth muscle function, the stomach can be divided into two distinct regions, a proximal region (i.e., all of the gastric fundus and approximately one-third of the oral gastric corpus), and a distal region [i.e., the remaining two-thirds of the gastric corpus, the antrum, and the gastro-duodenal junction (Kelly et al., 1981)]. Each region has a unique role in gastric function. The proximal stomach is mainly involved in the receipt and storage of ingested materials (Kelly et al., 1981; Camilleri, 2007). The distal stomach is mainly involved with retention and trituration of solid material; with prevention of reflux of substances from the duodenum (Kelly et al., 1981); and with regulation of emptying of liquids from the stomach (Collins et al., 1991; Anvari et al., 1995). These two distinct regions differ in their contractile

Corresponding Author: Richard A. Gillis, Department of Pharmacology, Georgetown University, 3900 Reservoir Rd., NW, Washington, DC 20057, Email: gillisr@georgetown.edu, Phone: 202-687-1607, Fax: (202)-687-2585.

Note: Preliminary data of this work were presented at the Society for Neuroscience Annual Meetings (2004, 2006).

Publisher's Disclaimer: This is a PDF file of an unedited manuscript that has been accepted for publication. As a service to our customers we are providing this early version of the manuscript. The manuscript will undergo copyediting, typesetting, and review of the resulting proof before it is published in its final citable form. Please note that during the production process errors may be discovered which could affect the content, and all legal disclaimers that apply to the journal pertain.

NIH-PA Author Manuscript
NIH-PA Author Manuscript
NIH-PA Author Manuscript

NIH-PA Author Manuscript

NIH-PA Author Manuscript

NIH-PA Author Manuscript

activity. The proximal stomach exhibits contractions that are primarily tonic in character whereas the distal stomach exhibits contractions that are mainly phasic in character (Kelly et al., 1981). One feature that the two regions have in common is their dependency on the vagus nerves for a significant part of the regulation of their contractile activity (Kelly et al., 1981).

In view of the separation of functions of the two parts of the stomach and in view of the importance of vagal influence over the contractility of the entire stomach, the question arises as to whether the CNS has the capacity to provide region-specific control over the proximal and distal regions of the stomach. Our recent published findings indicate that the brain does have this capacity through afferent inputs to the dorsal motor nucleus of the vagus (DMV), the hindbrain nucleus that contains most of the preganglionic vagal neurons that project to the stomach. Specifically, we have reported that two modes of stimulation of vago-vagal reflex pathways that inhibit the proximal stomach activate catecholaminergic neurons in the nucleus tractus solitarius (NTS) resulting in inhibition of DMV neurons to the proximal stomach (Ferreira et al., 2002, 2005). Indeed, in our first study addressing the question of CNS region-specific control over gastric function we reported that inhibition of gastric tone involved norepinephrine(NE)-induced inhibition of DMV gastric-projecting neurons whereas inhibition of phasic contractions involved GABA-induced inhibition of DMV gastric-projecting neurons (Ferreira et al., 2002). Approximately 60–70% of the inhibition in gastric tone was blocked by microinjecting alpha2-adrenoreceptor antagonists into the DMV, and approximately 80% of the inhibition of phasic contraction was blocked by microinjection a $GABA_A$ receptor antagonist into the DMV (Ferreira et al., 2002).

Our findings (Ferreira et al., 2002) that the fundus (gastric tone) can be regulated by a NTS noradrenergic pathway projecting to the DMV was confirmed and extended by Rogers and colleagues, 2003. These investigators activated a vago-vagal reflex that produced relaxation of the fundus. Associated with reflex activation was excitation of tyrosine hydroxylase-immunoreactive (TH-IR) neurons in the NTS. In addition, local brain application of alpha-adrenoreceptor antagonists counteracted reflex-induced gastric relaxation. The magnitude of antagonism was approximately 73%. Finally, microinjection of NE into the DMV mimicked the reflex-evoked relaxation of the fundus. The investigators suggested that noradrenergic neurons of the NTS played a prominent role in mediating the receptive relaxation reflex (Rogers et al., 2003). They did not pursue studies to determine whether noradrenergic neurons of the NTS play a similar role in vago-vagal reflex-induced inhibition of antrum motility.

Taken together, the above data suggest that selective reflex-induced engagement of the fundus might occur because noradrenergic neurons originating in the NTS make synaptic contact with DMV output neurons that project to the fundus but not to the antrum. This suggestion runs counter to the recent findings of Hayakawa et al., 2004, who examined the ultrastructure of catecholamine neurons in the DMV projecting to the rat stomach using double-label immunohistochemistry for tyrosine hydroxylase. Although their focus was on dopamine expressing neurons in the DMV, they do report that no TH-IR terminals were found in the DMV. The purpose of the present study was to examine whether noradrenergic neurons do, in fact, make contact with DMV neurons by injecting the retrograde tracer, CTβ-HRP, into the fundus or antrum. We then determined, with electron microscopy, whether noradrenergic terminals form synapses with DMV fundus-projecting neurons, but not with DMV antrum-projecting neurons. In addressing this idea we are also seeking an answer to the broader question of whether the CNS has the capacity to provide region-specific control over the proximal and distal regions of the stomach through engaging phenotypically different afferent inputs to the DMV.

NIH-PA Author Manuscript

NIH-PA Author Manuscript

NIH-PA Author Manuscript

4. MATERIALS AND METHODS

Retrograde Tracing Studies

Adult male Sprague-Dawley rats (275–325 g) (Taconic) were anesthetized with isoflurane by inhalation (4% induction, 1.5% maintenance mean alveolar concentration) and prepared for surgery. A 2 cm horizontal incision was made just below the ribcage. The stomach was gently lifted out of the peritoneal cavity and a 1% solution of the beta subunit of cholera toxin conjugated to horseradish peroxidase [CTβ-HRP, (List Biologicals)] was injected into the gastric smooth muscle of the fundus or antrum in 3–5 separate injections equaling a total volume of 2 μl. The approximate placement of injections is noted in the schematic shown as Figure 1. The stomach was re-inserted into the abdomen and the abdomen closed. Post-operatively, all rats received subcutaneous buprenorphine injections (0.02 mg/kg) at 12 hour intervals for 36 hours. Controls for the selectivity of the CTβ-HRP injection were as follows: 1) CTβ-HRP injection (2μl of a 1% solution) into the peritoneal cavity (n=2) (this resulted in zero labeling in the brainstem following a 48 hour survival period), and 2) CTβ-HRP injection (2ul of a 1% solution) into the tongue (n=2) (this resulted in histochemical label confined to the hypoglossal nucleus following a 48 hour survival period).

After a 48 hour survival period, animals were sacrificed under anesthesia (Nembutal 60 mg/kg, i.p.) by transcardiac perfusion with fixative. During this procedure, a gavage needle was threaded into the left ventricle and passed up into the proximal aorta. An incision was made into the right atrium to allow for fluid drainage, and approximately 100 ml of 1M phosphate buffered saline (PBS) followed by 150 ml fixative [2% paraformaldehyde (PF) + 3% acrolein in 1M PBS, pH 7.4] was infused into the left ventricle via a perfusion pump. The acrolein was flushed out with a final infused wash of 2% PF (100 ml). The brainstem and stomach were extracted and immersed in 2% PF for 30 minutes before transfer into 0.1M PBS for sectioning. We assured ourselves that the CTβ-HRP injection was made into either the fundus or the antrum and had not spread from one area to another by post-perfusion sectioning and histochemical processing (see below) of the stomach of each animal (total n=23). The number of animals used includes the 15 animals (n=8, fundus; n=7, antrum) for the retrograde tracing study and an additional 8 animals (n=4, fundus; n=4, antrum) for the ultrastructural study. Animals found to have CTβ-HRP present outside the injection site were not included in this analysis. Properly placed injections in the antrum or fundus were expected to mimic the results of Okumura et al., (1999) and Pagani et al., (1988). Both of these investigators noted a consistent medial-lateral distribution of retrogradely labeled neurons with antrum-projecting neurons located more medial than fundus-projecting neurons, and our results were similar (see Section 1 of RESULTS).

Assessment of the medial-lateral distribution of antrum and fundus-projecting neurons in the DMV was made by identifying the CTβ-HRP label in the DMV under light microscopy. Next, two measurements were taken from the midline of the coronal tissue section (center of the central canal). The first was from the central canal to the most medial CTβ-HRP labeled cell in that section and the second was from the central canal to the most lateral CTβ-HRP labeled cell. The distances for each of the two measurements were averaged and compared between animals with antrum label and animals with fundus label. Statistical comparisons were made using the Student's t-test. The criterion for statistical significance was $p < 0.05$.

To further characterize the populations of antrum or fundus-projecting neurons in the DMV, we also analyzed the same 25μm sections to study the rostral – caudal distribution of CTβ-HRP-labeled neurons. We counted the number of CTβ-HRP-labeled neurons in each 25 μm section spaced 125 μm apart, and the data appear in the histograms shown as figures 2d and 3d. From the total number of CTβ-HRP-labeled neurons for each animal, it was determined where 80% of the population was located and these areas are noted in figures 2e and 3e.

NIH-PA Author Manuscript

NIH-PA Author Manuscript

NIH-PA Author Manuscript

CTβ-HRP Histochemistry

Brainstems were sectioned on either a Leica SM2000R sliding microtome (Leica Instruments) into 25um coronal sections for light microscopic analysis or a Vibratome Series 1000 sectioning system (Technical Products International, Inc.) into 40um coronal sections for electron microscopy. Free-floating sections were processed to identify CTβ-HRP labeled entities by the tungstate stabilized tetramethylbenzidine (TMB) method of Weinberg and Van Eyck (1991), as described in detail by Llywellyn-Smith and Minson (1992). This method was performed at pH 6.0 and yields a crystalline reaction product which is readily detected in the electron microscope. Sections were preincubated for 20 minutes in a solution containing: 100ml of 0.1 M PBS, pH 6.0, 5.0 ml 1% ammonium paratungstate, 1.0 ml of 0.4% NH4CL, 1.0 ml 20% D-glucose, and 1.25 ml of 0.2% TMB free base in ethanol (Sigma). Subsequently, the sections were incubated in 100 ml of the same solution with the addition of 600 International Units (IU) of glucose oxidase. The development of the blue reaction product which is formed by the glucose oxidase reaction was monitored under a dissecting microscope and is typically complete within 20–30 minutes. The sections were washed 3 times in fresh 0.1 M phosphate buffer, pH 6.0, and then the reaction product was stabilized and enhanced with a cobalt chloride-diaminobenzidine-glucose oxidase reaction in a minor variation on the method of Rye et al. (1984). Briefly, tissues were incubated for 7 minutes in a solution containing: 100 ml 0.1 M phosphate buffer, pH 6.0, 100 mg diaminobenzidine, 1.0 ml NH4CL, 1.0 ml of 20% D-glucose, 2.0 ml of 1% cobalt chloride in water, and 600 IU of glucose oxidase. This second glucose oxidase reaction was terminated by washing in excess sodium phosphate buffer. Sections for light microscopy (25μm) were rinsed with PBS and mounted on glass slides for analysis. To analyze the distribution of antrum or fundus-projecting neurons, neurons in every 5^{th} section were counted and a total of labeled neurons for each animal was averaged and plotted (Fig. 2d,2e; Fig. 3d,3e). Sections for electron microscopy were rinsed in PBS and then processed immunocytochemically for the presence of either DβH or PNMT.

Immunocytochemistry

Brainstem sections were incubated for 30 minutes in a solution of 50% absolute ethanol in distilled water to enhance the penetration of antibodies throughout the tissue, followed by 3 washes in PBS. Tissues were then incubated in 0.1 M phosphate-buffered solution containing 1.0% bovine serum albumin (BSA) for 30 minutes and then incubated overnight in either mouse anti-DβH primary antiserum (Chemicon) diluted 1:30,000 in 0.1% BSA dissolved in 0.1 M PBS or rabbit anti-PNMT (Eugene Tech) diluted 1:4,000 in 0.1% BSA dissolved in 0.1 M PBS. The secondary antibody was either biotinylated anti-mouse made in horse (1:200) or biotinylated anti-rabbit made in goat (1:200) from Vector Laboratories. Sections were rinsed in PBS-BSA (0.1%) and then incubated for 1 hour in avidin-biotin peroxidase complex [1:50 in 0.1% PBS-BSA using the Vectastain ABC Elite kit followed by a glucose oxidase reaction utilizing DAB (100 mg DAB, 0.04% NH_4Cl, 0.2% D-glucose, 1200 IU glucose oxidase in 0.1M PBS)] to visualize the product. This reaction yields an amorphous electron dense reaction product when viewed in the electron microscope.

Processing for Electron Microscopy

Sections containing CTβ-HRP-labeled cells were processed for electron microscopy. These sections were further preserved in 2% osmium tetroxide for 1 hour, and rinsed with PBS. Free-floating sections were exposed to a graded series of dehydrations in ethanol and propylene oxide, and incubated overnight in a 1:1 propylene oxide:epon 812 plastic resin solution (Electron Microscopy Sciences). Tissues were flat-embedded between 2 sheets of aclar plastic (Ted Pella) and heated for 48 hours at 60° C. Embedded tissues were examined under a light microscope and the area of interest, the DMV, was cut out and re-embedded in Beem capsules which were filled with freshly prepared Epon 812 and heated for 48–72 hours at 60°C. The

NIH-PA Author Manuscript

NIH-PA Author Manuscript

NIH-PA Author Manuscript

hardened samples were removed from the oven and blocked for ultramicrotomy under a dissecting microscope (Nikon SMZ-U, Zoom 1–10). Blocks were cut on a Reichert Ultracut S ultramicrotome (Reichert, Leica Microsystems) into 70nm serial sections which were captured onto 300 mesh copper grids (Electron Microscopy Sciences) and double stained with uranyl acetate and lead citrate using a Leica EMStain Ultrastainer (Leica Microsystems). Sections were examined in a JEOL-JEM-1210 transmission electron microscope at 50 or 80 kV accelerating voltage.

Two 40μm sections from the intermediate DMV (this area includes DMV tissue beginning at the calamus scriptorius on the caudal end and extending +0.5 mm rostral) containing retrogradely labeled neurons from either the fundus or the antrum were examined. These sections were chosen because they contained the best combination of morphological preservation and histochemical/immunocytochemical labeling from each animal. From each 40 μm-thick section, 3 ultrathin sections separated by ~12 μm each were utilized for subsequent quantitative analysis. The spatial separation provided between samples insured the prevention of duplicate counts of the same terminal in our 3 samples throughout the neuropil. Ultrathin sections were examined at 8,000x magnification for the presence of the tungstate-TMB-generated crystalline reaction product. All retrogradely labeled profiles were photographed at 8,000x and 20,000x magnification. Synaptic contacts were examined in 20,000x magnification photographs taken of the entire circumference of all retrogradely labeled profiles. Photographic images were recorded using a Gatan Model 895 Ultra Scan 4000 CCD camera (Gatan, Warrendale, PA). Neuronal and dendritic profiles were identified according to previous ultrastructural descriptions (Peters et al., 1999; Gray, 1959, Massari et al., 2002). All terminals that made synaptic contact with retrogradely labeled neurons were identified and categorized as ‘labeled’ or ‘unlabeled’ based on the presence or absence of DβH (or PNMT) immunoreactivity (IR) in the terminal. These terminals were further characterized as either synaptic contacts or appositions. A synaptic contact is characterized by the presence of an electron-dense post-synaptic density and a pre-synaptic terminal with immunocytochemically-labeled vesicles which are located near the terminal membrane where it directly contacts the post-synaptic density. Appositions are an immunoreactive terminal which is located directly up against a CTβ-HRP-labeled profile but doesn’t possess an electron-dense post-synaptic density. It is presumed that some of these appositions actually do form synaptic contacts with the CTβ-HRP-labeled profile in a subsequent 70nm section. Each contact was then identified as either ‘axo-somatic’ or ‘axo-dendritic’ and either symmetric or asymmetric based on previously reported definitions(Peters et al., 1999).

The total number of profiles which contained CTβ-HRP retrograde labeling is expressed in Tables 1 and 2 and is the combined total of each animal added together. The same method was used to obtain figures for the total synaptic contacts and total appositions shown in Tables 1 and 2. The percent of synapses (or appositions) formed between retrogradely labeled profiles and immunoreactive terminals was calculated for each animal from a total of the synaptic contacts for that animal. The individual percentages for each animal were then averaged with the percentages of other animals in the experimental group to yield the data expressed in Table 1 (DβH-IR with fundus or antrum-projecting neurons) and Table 2 (PNMT-IR with fundus-projecting neurons). Average values for these data are presented as means +/− SEM. Statistical comparisons were made using the Student’s t-test. The criterion for statistical significance was $p < 0.05$.

NIH-PA Author Manuscript

NIH-PA Author Manuscript

NIH-PA Author Manuscript

5. RESULTS

I. Light Microscopic Analysis of the DMV after injection of CTβ-HRP into either the Fundus or the Antrum

In all animals that received injection of CTβ-HRP into either the fundus or the antrum, a column of retrogradely labeled neurons was observed bilaterally in the DMV. Representative coronal sections showing typical neuronal label in the DMV from the fundus injection appear as Figure 2(a–c). At −0.5mm [zero point is the calamus scriptorius (cs)], CTβ-HRP label is present but not robust (Fig. 2a). At + 0.55mm rostral to the cs, CTβ-HRP injected into the fundus is extremely dense (Fig. 2b). At + 0.75mm rostral to the cs, the CTβ-HRP label is still present, but appears much less dense than that at + 0.55mm rostral to the cs (Fig. 2c). The DMV was the only brainstem area to be labeled by CTβ-HRP injection into the fundus.

The retrograde tracing data involving the 8 rats receiving CTβ-HRP injections into the fundus appear in the histograms shown as figure 2d. As can be noted, the most intense labeling occurred from + 0.125 mm to, and including, +0.50 mm rostral to cs. Indeed, 80% of all labeled DMV neurons were contained in the area − 0.125 to + 0.50 mm on either side of cs (i.e., within a 625 μm span of the DMV).

Representative coronal sections showing typical neuronal label in the DMV from the antrum injection appear as figure 3(a–c). Similar to the distribution of label in the DMV after fundus injection, we found a light label present at − 0.5mm caudal to the cs (Fig. 3a), a very dense label at + 0.55 mm rostral to the cs (Fig. 3b), and a tapering off of the CTβ-HRP label intensity at + 0.75 mm rostral to the cs (Fig. 3c). Again, the DMV was the only brainstem area to be labeled by CTβ-HRP injection into the antrum.

The retrograde tracing data involving the 7 rats receiving CTβ-HRP injections into the antrum appear in the histogram shown as figure 3d. As can be noted, the most intense labeling occurred from cs to, and including, +0.75 mm rostral to cs. Indeed, 80% of all labeled DMV neurons were contained in the area between cs and + 0.75 mm rostral to cs (i.e., within a 750 μm span of the DMV).

In performing the above analysis we also observed that fundus projecting DMV neurons were generally located more lateral from the midline as compared to the antrum projecting DMV neurons. This observation has also been made by other investigators in the rat (e.g., Okumura et al., 1999), and by us in the cat (Pagani et al., 1988). In the present study we analyzed the medial-lateral distribution of DMV labeled neurons at 4 caudal – rostral levels, namely, caudal to the cs, cs, +0.5 mm rostral to the cs, and rostral to the area postrema. These data appear in the histograms displayed in figure 2e (fundus) and figure 3e (antrum). Statistical analysis of these data indicated that antrum-projecting neurons were more medial than fundus-projecting neurons at the caudal, cs, and +0.5 mm rostral to cs levels, ($p < 0.05$) but not at the part of the DMV rostral to the area postrema ($p > 0.05$).

The most important finding of these studies is that the results identified the locations of the highest number of DMV neurons that project to the fundus and antrum. Thus, the area from the cs to + 0.5 mm rostral to the cs and just medial to the midline contained the highest number of cells projecting to the antrum. The area from the cs to + 0.5 mm rostral to the cs and just lateral to the column of antrum-projecting neurons contained the highest number of cells projecting to the fundus. This is the region of the DMV where ultrathin sections were taken for electron microscopic analysis of catecholaminergic synapses.

NIH-PA Author Manuscript

NIH-PA Author Manuscript

NIH-PA Author Manuscript

II. Electron Microscopic Analysis

First, we focused on DMV preganglionic parasympathetic neurons that innervate the fundus and DβH-IR terminals in the DMV. Tissue examined was in the region of the DMV from cs to + 0.5mm rostral to this landmark as defined by our CTβ-HRP study. Retrograde label from CTβ-HRP injected into the fundus was readily observed in perikarya, proximal and distal dendrites, and myelinated axons by the presence of a crystalline TMB-tungstate reaction product (Fig. 5). Perikaryas were similar to those described by Hayakawa et al., (2004) and McLean and Hopkins (1981) in their electron microscopic studies of the DMV of the rat and cat, respectively. Perikarya were small or medium-sized, round or oval shaped, and contained a nucleolus, numerous mitochondria, rough endoplasmic reticulum, Golgi apparatuses, and lysosomes. An average of approximately 1.7–2.0 synaptic contacts with each soma and/or dendrite per section was observed in CTβ-HRP labeled perikarya of the rat DMV.

DβH-IR was found within the part of the DMV examined (i.e., cs to 0.5mm rostral to cs). Immunoreactivity could be identified as an electron-dense, amorphous DAB reaction product in the electron microscope, and was found in nerve terminals (Fig. 4a), unmyelinated axons, dendrites (Fig. 4b), and perikarya. DβH-IR terminals formed both axo-dendritic (Fig. 5) and axo-somatic (data not shown) synaptic contacts with CTβ-HRP labeled dendrites and perikarya, as well as many appositions (Fig. 5, Table 1). DβH-IR terminals contained an assortment of numerous small, clear, round or pleomorphic vesicles (Figs. 4a & 5a, 5b). Some DβH-IR terminals also contained several large, dense core vesicles (Figs. 4a & 5c). DβH-IR terminals formed mostly symmetric synapses, although a few asymmetric synapses were also observed (Fig. 5). Unlabeled terminals that formed synapses with DMV CTβ-HRP labeled neurons all contained an assortment of small, clear, round or pleomorphic vesicles and many also contained large, dense core vesicles (Fig. 5). These terminals also made both symmetric and asymmetric synapses (Fig. 5).

From a pooled total of 482 synaptic contacts with retrogradely labeled dendritic and somatic profiles, 17.4 +/− 2.7% were DβH-IR (Table 1). The proportion of DβH-IR terminals that formed axo-dendritic synapses (approximately 91%) was significantly higher than the proportion that formed axo-somatic synapses (approximately 9%), ($p < 0.05$). The percentage of 17.4 +/− 2.7% may have been as under-estimation because the examination of the brain tissue revealed many appositions with retrogradely labeled profiles, and the percent of appositions with DβH-IR was 14.2 +/− 2.1% (Table 1). Finally, we observed that DβH-IR terminals also formed contacts with unlabeled profiles in the DMV.

Next, we focused on DMV preganglionic parasympathetic neurons that innervate the antrum and DβH-IR terminals in the DMV. Tissue examined was again the part of the DMV as defined by our CTβ-HRP study (i.e., cs to 0.5mm rostral to cs). The appearance of retrograde label from CTβ-HRP injected into the antrum was similar to that seen for the fundus studies. Similarly, DβH-IR was also distributed in the DMV as described for the fundus innervation studies above. DβH-IR terminals formed synapses with only unlabeled, antrum-projecting neurons in the DMV (Fig 6). From a pooled total of 384 synaptic contacts with retrogradely labeled dendrites and somatic profiles, none of the 384 synapses examined involving the dendrites or perikarya of DMV antrum-projecting neurons was immunoreactive for DβH (Fig. 6, Table 1).

The total number of appositions with retrogradely labeled profiles was also examined. Only 1 possible apposition was noted (Table 1), and this apposition was of the axo-dendritic type. Many unlabeled terminals did form synapses with CTβ-HRP labeled profiles that were identified from injecting the retrograde tracer into the antrum (Fig. 6). The profiles retrogradely labeled from the antrum were rarely detected in the vicinity of DβH-IR terminals, however, one such terminal is shown in figure 6b.

NIH-PA Author Manuscript

NIH-PA Author Manuscript

NIH-PA Author Manuscript

We also examined the DMV for evidence of PNMT-IR terminals forming synaptic contacts with DMV fundus-projecting neurons. Like DβH-IR, PNMT-IR could be detected as an electron-dense DAB reaction product in the electron microscope, and was found in terminals (Fig. 4c), unmyelinated axons, dendrites, and perikarya (data not shown). Also, like DβH-IR terminals, PNMT-IR terminals formed both axo-dendritic (approximately 96%) and axo-somatic (approximately 4%) synaptic contacts with CTβ-HRP labeled dendrites and perikarya, as well as many appositions (Table 2). All PNMT-IR terminals appeared to contain a similar mixture of small, clear, round or pleomorphic vesicles and many also contained several large, dense core vesicles (Figs. 4c & 7) as noted with DβH-IR terminals. PNMT-IR terminals formed symmetric synapses (data not shown).

From a pooled total of 325 synaptic contacts with retrogradely labeled dendritic and somatic profiles, 4.4 +/− 1.5% were PNMT-IR (Table 2). The percentage of 4.4 +/− 1.5% may have been an underestimation because examination of the brain tissue revealed appositions with retrogradely labeled profiles and the percent of appositions with PNMT-IR terminals was 1.2 +/− 2.3% (Table 2).

Evidence of PNMT-IR terminals synapsing with DMV antrum-projecting neurons was not looked for because no DβH-IR terminals synapsing with DMV antrum-projecting neurons were observed (Table 1).

6. DISCUSSION

Our two earlier DMV drug microinjection studies (Ferreira et al., 2002, 2005) and our c-fos/tyrosine hydroxylase NTS immunocytochemical study (also described in Ferreira et al., 2005) suggested to us that vago-vagal reflex-induced inhibition of the proximal stomach (i.e., fundus) of the rat was due in large part to activation of second order hindbrain catecholaminergic projection neurons to the DMV. Data from the first of our two studies (Ferreira et al., 2002) suggested to us that the catecholaminergic neural projection to the DMV was not mediating vago-vagal reflex-induced inhibition of the distal stomach (i.e., antrum); instead, this reflex-evoked response appeared to be mediated by second order hindbrain GABAergic projection neurons to the DMV. The purpose of our present study was to use electron microscopy to determine whether catecholaminergic terminals form synapses with DMV fundus-projecting neurons, but not with DMV antrum-projecting neurons.

Using the electron microscope, we have provided visual evidence for the existence of synaptic contacts between fundus-projecting DMV neurons and DβH-IR terminals. The vast majority of synaptic contacts between fundus-projecting profiles and DβH-IR terminals were axo-dendritic. In our quantitative analysis of neurons which project to the fundus, we found that of all the synapses observed with these neurons, 17.4 +/− 2.7% contain DβH-IR. This percentage is very similar to the data of others (Moore et al., 2004) regarding evidence for a significant afferent input to a hindbrain parasympathetic nucleus (nucleus ambiguous) projecting to, and controlling airway function. Most important, since alpha-adrenoreceptor antagonist applied locally to the DMV counteracted all but 25–40% of reflex-induced inhibition of gastric tone (Ferreira et al., 2002; Rogers et al., 2003), we would suggest that the largest part of this response is mediated by just 17.4 +/− 2.7% of the synapses at fundus-projecting neurons.

In addition, using the electron microscope, we found no synaptic contact between antrum-projection neurons and DβH-IR terminals. Ultrastructurally, fundus and antrum-projecting neurons and dendrites looked the same, and received an average of 1.7–2.0 synaptic contacts with terminals (this number includes the total number of synapses, both DβH-IR and unlabeled synapses per section). The only obvious difference we observed during our ultrastructural

NIH-PA Author Manuscript

NIH-PA Author Manuscript

NIH-PA Author Manuscript

analysis between the fundus and antrum-projecting neurons was that the fundus received catecholaminergic input and the antrum did not.

The hindbrain contains separate neuronal systems that utilize norepinephrine and epinephrine (Dahlstrom and Fuxe, 1964; Hokfelt et al., 1973, 1974), and Siaud and colleagues, 1990, have previously reported ultrastructural evidence for epinephrine containing nerve terminals forming synaptic contacts with DMV neurons projecting to the “fundus region” of the rat stomach. Ultrastructural evidence was based on immunoreactivity to the enzyme that N-methylates norepinephrine, thus forming epinephrine, namely PNMT. Since epinephrine containing neurons also exhibit DβH-IR, we needed to clarify whether the DβH-IR terminals described above synapsing with fundus-projecting neurons were just a confirmation of the earlier findings of Siaud et al., 1990, regarding epinephrine neuronal input to the DMV. In our quantitative analysis of neurons which project to the fundus, we found that of all the synapses observed with these neurons, only 4.4 +/− 1.5% contained PNMT-IR. This percentage was only one-fourth of the percentage of synapses that contained DβH-IR, suggesting that in addition to confirming the findings of Siaud and colleagues, 1990, we have obtained new evidence for the fundus receiving noradrenergic input [Note: we assume that the sensitivity of the antibodies for DβH and PNMT are similar]. Siaud and colleagues, 1990, did not study PNMT-IR in synapses with DMV neurons projecting to the antrum. We also did not examine this issue since antrum-projecting neurons did not receive DβH terminals, and it is well established that neurons that synthesize epinephrine require norepinephrine as a precursor (Kirschner, 1959).

In addition to the 4-fold higher percentage of synapses that contain DβH-IR as compared to synapses that contain PNMT-IR, there is another compelling reason that indicated that fundus-projecting neurons receive noradrenergic input. It is based on our earlier evidence that the catecholaminergic synapses that we studied are an integral part of the vago-vagal fundus relaxation reflex (Ferreira et al., 2002, 2005). Nicotine given i.v. can activate the neural pathway that underlies this reflex (Ferreira et al., 2002, 2005), as can esophageal distension (Rogers et al., 2003; Ferreira et al., 2005). Immunocytochemical techniques showed that reflex activation was associated with excitation of TH-IR neurons in the medial and centralis subnuclei of the nucleus tractus solitarius (NTS) (Ferreira et al., 2005; Rogers et al., 2003). TH-IR was not proof that NTS noradrenergic neurons were activated because it is a marker for dopamine, norepinephrine and epinephrine neurons. However, the TH-containing cells were located in the NTS from the cs to + 0.90 mm rostral to the cs (Ferreira et al., 2005). The A2 norepinephrine group of neurons corresponds anatomically to this rostrocaudal region of the NTS (Kalia et al., 1985; Paxinos et al., 1999)]. [The location of the well-known epinephrine group of neurons, C2, are located farther rostral than the A2 norepinephrine group of neurons (Kalia et al., 1985; Paxinos et al., 1999)]. Thus, we concluded that the TH-IR NTS neurons activated in rats subjected to esophageal distension and to i.v. nicotine were most likely noradrenergic (Ferreira et al., 2005).

Additional evidence that it is a primarily noradrenergic input, rather than an epinephrine input, to the fundus-projecting neurons are the findings of Sumal et al., 1983, who demonstrated that A2 noradrenergic neurons within the NTS are innervated by terminals from first-order vagal afferent neurons in the nodose ganglion. Furthermore, Moore and Guyenet, 1983, showed that vagal afferent nerve stimulation affects the firing rate of A2 neurons. Additionally, electrical stimulation of the A2 noradrenergic cell group produces inhibitory postsynaptic potentials (IPSP’s) in the DMV, which were antagonized by the α2-adrenoreceptor antagonist yohimbine (Fukuda et al., 1987). This also has been shown to be true with some spontaneously recorded IPSP’s at the DMV (Fukuda et al., 1987). Consistent with the presence of α2-adrenoreceptors on DMV neurons were the descriptions of α2a-adenergic receptor-like IR (Talley et al.,

NIH-PA Author Manuscript

NIH-PA Author Manuscript

NIH-PA Author Manuscript

1996) and α2c-adrenergic receptor-like IR rat (Rosin et al., 1996) located on neurons within the neuropil of the DMV.

Taken together, all these cited points indicate that the A2 norepinephrine neurons in the NTS are the important source of the DβH-IR terminals synapsing with fundus-projecting neurons. Other sources of these terminals may exist and the one source that stands out as a possible contributor is the A6 noradrenergic cell group (i.e., locus coeruleus). Ter Horst et al., 1991, reported that an injection of anterograde tracer into the locus coeruleus can be found in the general area of the DMV where we found DβH-IR terminals. Card et al., 1990, showed that the transynaptic retrograde tracer, Pseudorabies virus, injected into the corpus of the stomach resulted in the appearance of virus in the DMV 64 hours post-injection, and in the locus coeruleus 70 hours post-injection. Lastly, stimulation of locus coeruleus neurons produced vagus nerve-mediated decreases in gastric motility (Osumi et al., 1981).

In view of our current electron microscopic evidence of DβH-IR terminals synapsing with DMV fundus-projecting neurons, in view of evidence of others indicating that A2 noradrenergic neurons play a role in a vago-vagal reflex pathway (Rogers et al., 2003; Kalia et al., 1985; Sumal et al., 1983; Moore and Guyenet, 1983; Fukuda et al., 1987, Talley et al., 1996; Rosin et al., 1996), and in view of our previous DMV α2-drenoreceptor antagonist microinjection data plus c-fos/TH-IR data (Ferreira et al., 2002, 2005), we propose that norepinephrine is a key hindbrain inhibitory neurotransmitter in a vago-vagal reflex pathway that controls fundus smooth muscle. Most DβH-IR terminals synapsing with DMV fundus-projecting neurons were of the symmetric type which is characteristic of an inhibitory synapse (Peters et al., 1999). The DβH-IR terminals observed contained an assortment of numerous small, clear, round or pleomorphic vesicles, and some DβH-IR terminals also contained large dense-core vesicles. Both types of vesicles have been reported to store catecholamines (De Camilli and Jahn, 1990; Merighi et al., 1991), though Nirenberg et al., 1995, provided evidence suggesting that monoamines in the NTS were stored primarily in dense core vesicles (Nirenberg et al., 1995).

Our finding of no DβH-IR terminals synapsing with DMV antrum-projecting neurons indicate that vago-vagal reflexes controlling this portion of the stomach involves a neurotransmitter other than norepinephrine. Studies are in progress to elucidate the identity of this neurotransmitter. Taken together, the data of the present study are consistent with our hypothesis that the CNS has the capacity to provide region-specific control over the proximal (fundus) and distal (antrum) stomach through engaging phenotypically different efferent inputs to the DMV.

Acknowledgements

Grant Support: NIH grant #'s: R01DK57105 (RAG), R01DK56925 (RAG), R24MH067627 (VJM), U54NS039407 (VJM), and F31NS049786 (RJP)

References

1). Anvari M, Yu P, Dent J, Jamieson GG. Role of antral intramural neural pathways in control of gastric emptying in the pig. J Physiol 1995;488:203–209. [PubMed: 8568656]

2). Cammilleri M. Diabetic Gastroporesis. New Engl J Med 2007;356:820–829. [PubMed: 17314341]

3). Card JP, Rinaman L, Schwaber JS, Miselis RR, Whealy ME, Robbins AK, Enquist LW. Neurotropic properties of psuedorabies virus: uptake and transneuronal passage in the rat central nervous system. J Neurosci 1990;10:2400–2411. [PubMed: 2115911]

4). Collins PJ, Houghton LA, Read NW, Horowitz M, Chatterton BE, Heddle R, Dent R. Role of the proximal and distal stomach in mixed solid and liquid meal emptying. Gut 1991;32:615–619. [PubMed: 2060870]

NIH-PA Author Manuscript

NIH-PA Author Manuscript

NIH-PA Author Manuscript

5). Dahlstrom A, Fuxe K. Evidence for the existence of monoamine containing neurons in the central nervous system. 1. Demonstration of monoamines in the cell bodies of brainstem neurons. Acta Physiol Scand Suppl 1964;62:1–55.

6). De Camilli P, Jahn R. Pathways to regulated exocytosis in neurons. Annu Rev Physiol 1990;52:625–645. [PubMed: 2184771]

7). Ferreira M Jr, Sahibzada N, Shi M, Panico W, Neidringhaus M, Wasserman A, Kellar KJ, Verbalis J, Gillis RA. CNS site of action and brainstem circuitry responsible for the intravenous effects of nicotine on gastric tone. J Neurosci 2002;22:2764–2779. [PubMed: 11923442]

8). Ferreira M Jr, Sahibzada N, Shi M, Niedringhaus M, Wester MR, Jones AR, Verbalis JG, Gillis RA. Hindbrain chemical mediators of reflex-induced inhibition of gastric tone produced by esophageal distension and intravenous nicotine. Am J Physiol Regul Integr Comp Physiol 2005;289:R1482–R1495. [PubMed: 16051723]

9). Fukuda A, Minami T, Nabekura J, Oomura Y. The effects of noradrenaline on neurons in the rat dorsal motor nucleus of the vagus, in vitro. J Physiol 1987;393:213–231. [PubMed: 2895810]

10). Gray EG. Axo-somatic and axo-dendritic synapses of the cerebral cortex: an electron microscopic study. J Anat 1959;93:420–433. [PubMed: 13829103]

11). Hayakawa T, Takanaga A, Tanaka K, Maeda S, Seki M. Distribution and ultrastructure of dopaminergic neurons in the dorsal motor nucleus of the vagus projecting to the stomach of the rat. Brain Res 2004;1006:66–73. [PubMed: 15047025]

12). Hokfelt T, Fuxe K, Goldstein M, Johansson O. Evidence for adrenaline neurons in the rat brain. Acta Physiol Scand 1973;89:286–288. [PubMed: 4128798]

13). Hokfelt T, Fuxe K, Goldstein M, Johansson O. Immunohistochemical evidence for the existence of adrenaline neurons in the rat brain. Brain Res 1974;66:235–251.

14). Hopkins DA, Bieger D, de Vente J, Steinbusch WM. Vagal efferent projections: viscerotopy, neurochemistry and effects of vagotomy. Prog Brain Res 1996;107:79–96. [PubMed: 8782514]

15). Kalia M, Fuxe K, Goldstein M. Rat medulla oblongata. II. Dopaminergic, noradrenergic (A1 and A2) and adrenergic neurons, nerve fibers, and presumptive processes. J Comp Neurol 1985;233:308–332. [PubMed: 2858497]

16). Kelly, KA. Motility of the Stomach and Gastroduodenal Junction. In: Johnson, LR., editor. Physiology of the Gastronintestinal Tract. 1. 1. Raven Press; New York: 1981. p. 393-410.

17). Kirshner N. Biosynthesis of adrenaline and noradrenaline. Pharmacol Rev 1959;11:350–357. [PubMed: 13667414]

18). Llewellyn-Smith IJ, Minson JB. Complete penetration of antibodies into vibratome sections after glutaraldehyde fixation and ethanol treatment: light and electron microscopy for neuropeptides. J Histochem Cytochem 1992;40:1741–1749. [PubMed: 1431060]

19). Massari VJ, Haxhiu MA. Substance P afferent terminals innervate vagal preganglionic neurons projecting to the trachea of the ferret. Auton Neurosci 2002;96:103–112. [PubMed: 11958475]

20). McLean JH, Hopkins DA. A light and electron microscopic study of the dorsal motor nucleus of the vagus nerve in the cat. J Comp Neurol 1981;195:157–175. [PubMed: 7204650]

21). Merighi A, Polak JM, Theodosis DT. Ultrastructural visualization of glutamate and aspartate immunoreactivites in the rat dorsal horn, with special reference to the co-localization of glutamate, substance P and calcitonin-gene related peptide. Neurosci 1991;40:67–80.

22). Moore SD, Guyenet PG. Alpha-receptor mediated inhibition of A2 noradrenergic neurons. Brain Res 1983;276:188–91. [PubMed: 6138124]

23). Moore CT, Wilson CG, Mayer CA, Acquah SS, Massari VJ, Haxhiu MA. A GABAergic inhibitory microcircuit controlling cholinergic outflow to the airways. J Appl Physiol 2004;96:260–270. [PubMed: 12972437]

24). Nirenberg MJ, Liu Y, Peter D, Edwards RH, Pickel VM. The vesicular monoamine transporter 2 is present in small synaptic vesicels and preferentially localizes to large dense core vesicles in rat solitary tract nuclei. Proc Natl Acad Sci USA 1995;92:8773–8777. [PubMed: 7568015]

25). Okumura T, Namiki M. Vagal motor neurons innervating the stomach are site-specifically organized in the dorsal motor nucleus of the vagus nerve in rats. J Autonomic Nervous System 1999;29:157–162.

NIH-PA Author Manuscript

NIH-PA Author Manuscript

NIH-PA Author Manuscript

26). Osumi Y, Ishikawa T, Okuma Y, Nagasaka Y, Fujiwara M. Inhibition of gastric functions by stimulation of the rat locus coeruleus. Eur J Pharmacol 1981;75:27–35. [PubMed: 7318897]

27). Pagani FD, Norman WP, Gillis RA. Medullary parasympathetic innervate specific sites in the feline stomach. Gastroenterology 1988;95:277–288. [PubMed: 3391362]

28). Paxinos, G.; Carrive, P.; Wang, H.; Wang, P. Chemoarchitecture Altas of The Rat Brainstem. Academic Press; San Diego: 1999.

29). Peters, A.; Palay, SL.; Webster, HD. The Fine Structure of the Nervous System. Oxford University Press; New York: 1999.

30). Rogers RC, Travagli RA, Hermann GE. Noradrenergic neurons in the rat solitary nucleus participate in the esophageal-gastric relaxation reflex. Am J Physiol Regul Integr Comp Physiol 2003;285:R479–R489. [PubMed: 12714355]

31). Rosin DL, Talley EM, Lee A, Stronetta RL, Gaylinn BD, Guyenet PG, Lynch KR. Distribution of $\alpha 2_C$-adrenergic receptor-like immunoreactivity in the rat central nervous system. J Comp Neurol 1996;372:135–65. [PubMed: 8841925]

32). Rye DB, Saper CB, Wainer BH. Stabilization of the tetramethylbenzidine (TMB) reaction product: application for retrograde and anterograde tracing, and combination with immunohistochemistry. J Histochem Cytochem 1984;32:1145–1153. [PubMed: 6548485]

33). Siaud P, Pucch R, Assenmacher I, Alonso G. Adrenergic innervation of the dorsal vagal motor nucleus: possible involvement in inhibitory control of gastric acid and pancreatic insulin secretion. Cell Tissue Res 1990;259:535–542. [PubMed: 2180575]

34). Sumal KK, Blessing WW, Joh TH, Reis DJ, Pickel VM. Synaptic interaction of vagal afferents and catecholaminergic neurons in the rat nucleus tractus solitarius. Brain Res 1983;277:31–40. [PubMed: 6139145]

35). Talley EM, Rosin DL, Lee A, Guyenet PG, Lynch KR. Distribution of $\alpha 2_A$-adrenergic receptor-like Immunoreactivity in the rat central nervous system. J Comp Neurol 1996;372:111–134. [PubMed: 8841924]

36). Ter Horst GJ, Toes GJ, Van Willigen JD. Locus Coeruleus projections to the dorsal motor nucleus in the rat. Neurosci 1991;45:153–160.

37). Weinberg WJ, van Eyck SL. A tetramethylbenzidine/tungstate reaction for horseradish peroxidase histochemistry. J Histochem Cytochem 1991;38:1143–1148. [PubMed: 1906909]

Abbreviations

DβH
: dopamine-beta-hydroxylase

PNMT
: phenylethanolamine-N-methyltransferase

IR
: immunoreactive

TH
: tyrosine hydroxylase

DMV
: dorsal motor nucleus of the vagus

NTS
: nucleus tractus solitarius

cs
: calamus scriptorius

EPI
: epinephrine

NIH-PA Author Manuscript

NIH-PA Author Manuscript

NIH-PA Author Manuscript

NE

norepinephrine

CTβ-HRP

cholera toxin beta subunit conjugated to horseradish peroxidase

NIH-PA Author Manuscript

NIH-PA Author Manuscript

NIH-PA Author Manuscript

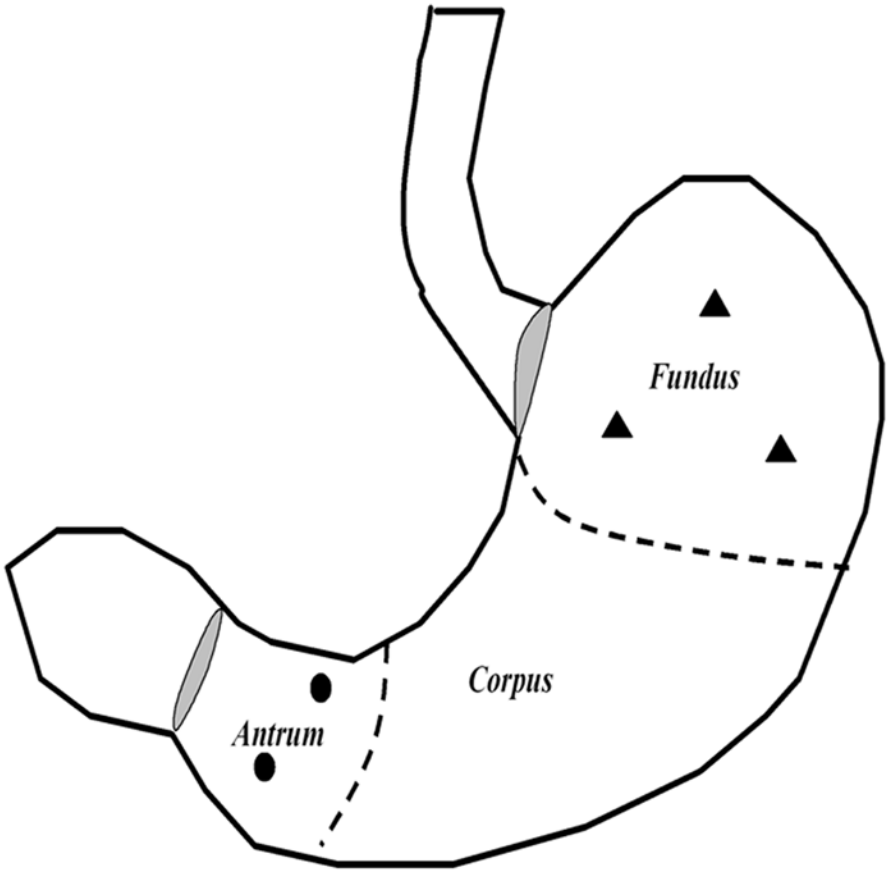

Figure 1.
Schematic representation of the anterior aspect of the stomach indicating the sites which received an injection of CTβ-HRP into the fundus (triangles) or antrum (circles). Each animal received a total of 2μl of 1% CTβ-HRP over 3–5 injection sites. Injections were made in both the anterior and the posterior sides to produce a bilateral DMV label.

NIH-PA Author Manuscript
NIH-PA Author Manuscript
NIH-PA Author Manuscript

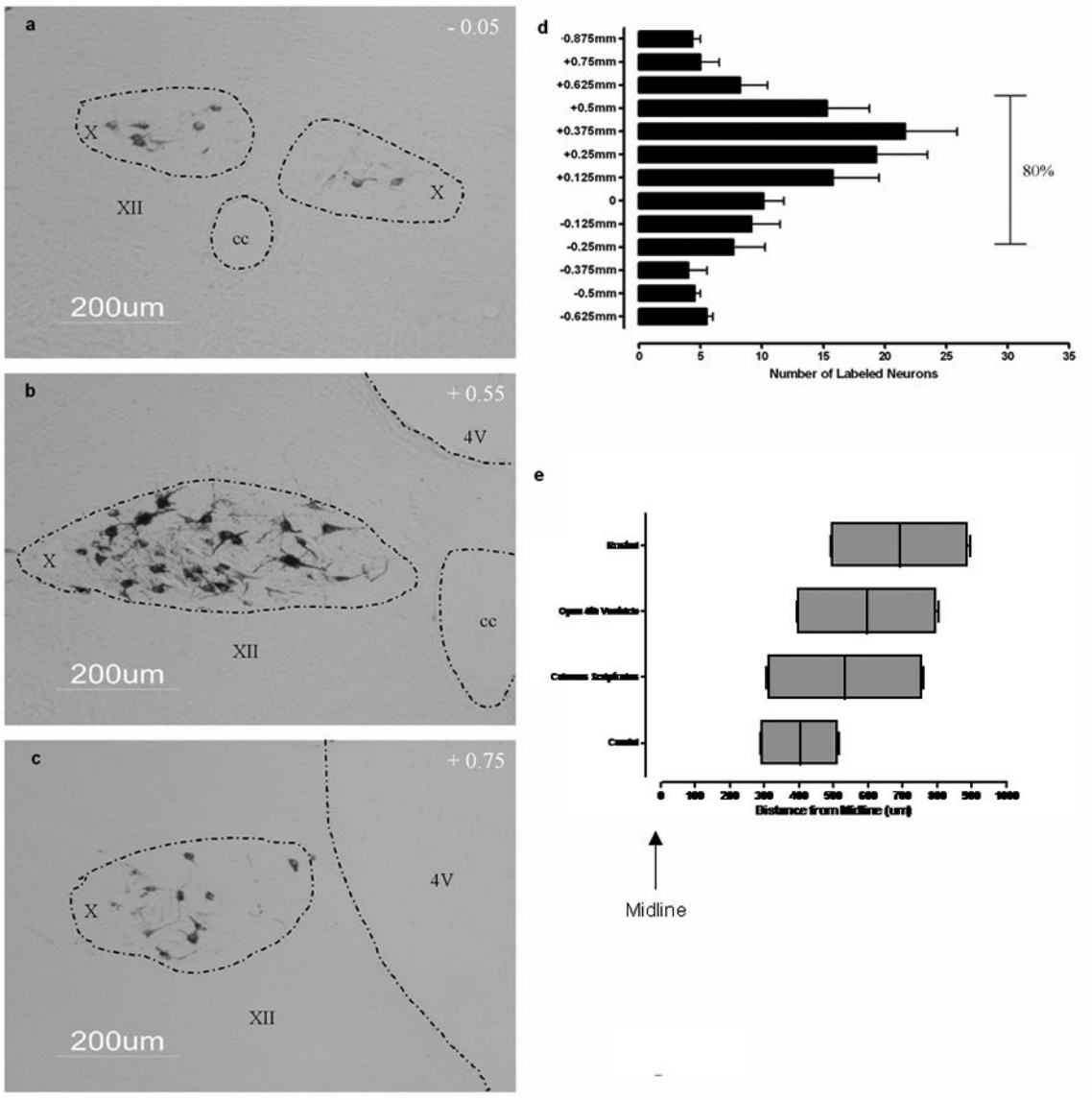

Figure 2.

CTβ-HRP retrograde labeling in the DMV resulting from injection of CTβ-HRP into the fundus of the stomach. 1 (a–c): Retrograde label from the fundus as seen in the light microscope at −0.05mm (1a), + 0.55mm (1b), and + 0.75 mm (1c) is readily identified by the presence of dark crystalline tetramethylbenzidine (TMB)-tungstate reaction product. 1d) Rostral – caudal distribution (i.e., vertical axis) of neurons retrogradely labeled from the fundus. 1e) Medial – lateral distribution of neurons retrogradely labeled from the fundus. All coordinates were calculated based on 0 = calamus scriptorius (cs). X: DMV, XII: Hypoglossal Nucleus, cc: central canal, 4V: fourth ventricle.

NIH-PA Author Manuscript

NIH-PA Author Manuscript

NIH-PA Author Manuscript

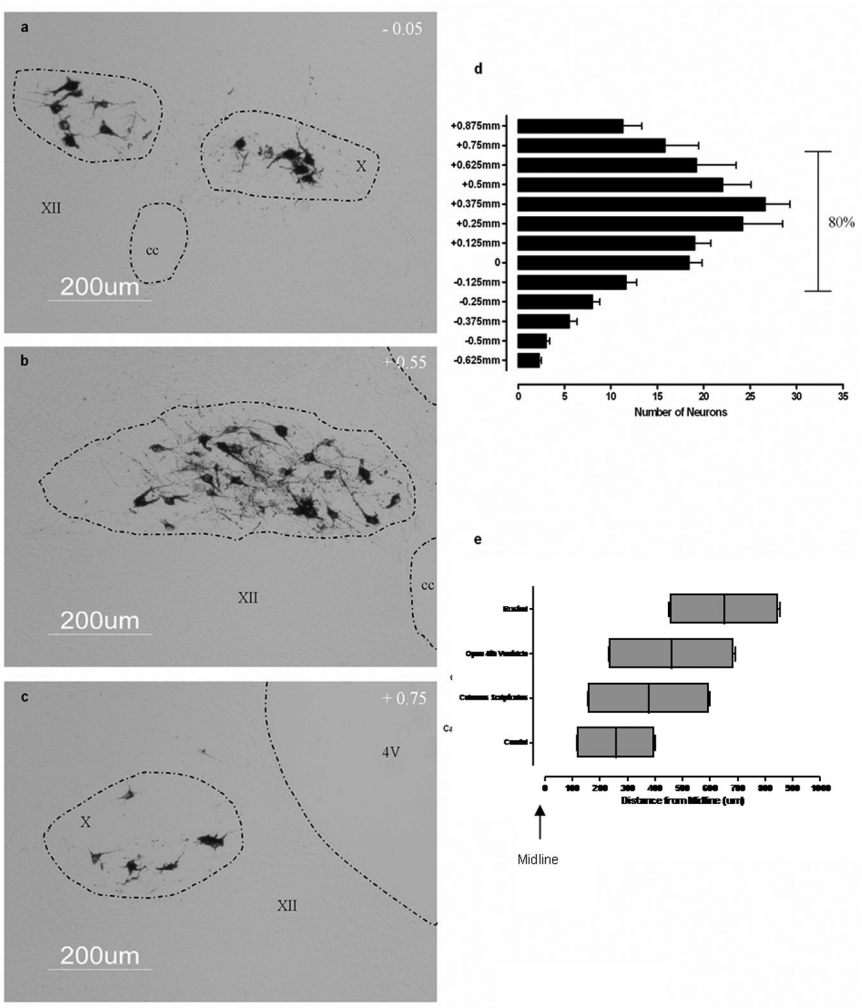

Figure 3.

CTβ-HRP retrograde labeling in the DMV resulting from injection of CTβ-HRP into the antrum of the stomach. 1 (a–c): Retrograde label from the antrum as seen in the light microscope at −0.05mm (1a), + 0.55mm (1b), and + 0.75 mm (1c) is readily identified by the presence of dark crystalline tetramethylbenzidine (TMB)-tungstate reaction product. 1d) Rostral – caudal distribution (i.e., vertical axis) of neurons retrogradely labeled from the antrum. 1e) Medial – lateral distribution of neurons retrogradely labeled from the antrum. All coordinates were calculated with 0 = calamus scriptorius. X: DMV, XII: Hypoglossal Nucleus, cc: central canal, 4V: fourth ventricle.

NIH-PA Author Manuscript
NIH-PA Author Manuscript
NIH-PA Author Manuscript

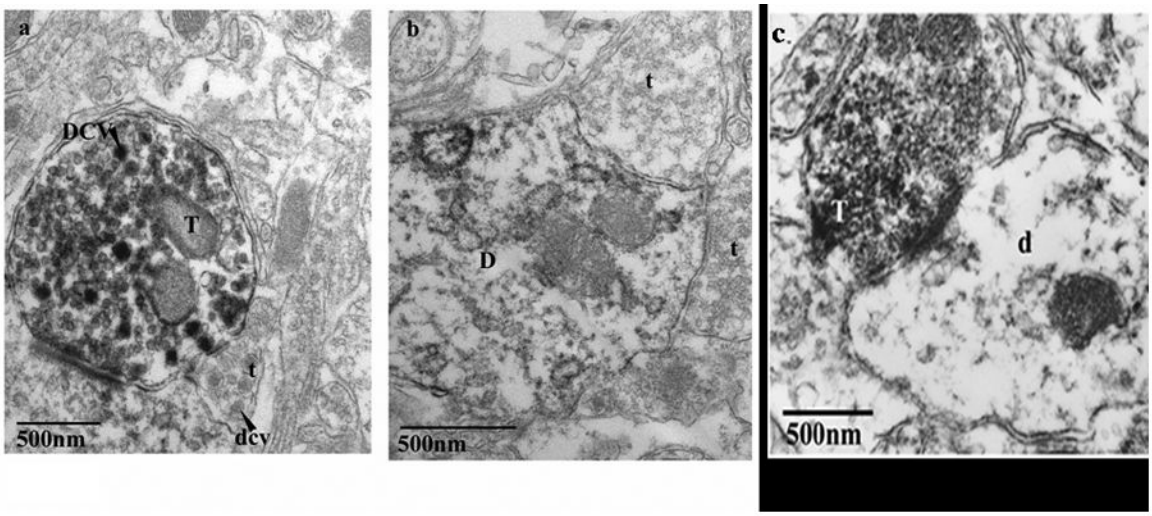

Figure 4.

DβH and PNMT-IR at the ultrastructural level. 4a) DβH-IR is readily detected as a dark, amorphous, diaminobenzidine (DAB) reaction product. Note that the DβH-IR terminal (T) contains a mixed population of mostly small, clear, pleomorphic vesicles and dense core vesicles (DCV: labeled, dcv: unlabeled, arrowheads). An unlabeled terminal (t) is identified for comparison. 4b) DβH-IR was also noted in numerous dendrites (D). 4c) PNMT-IR is also readily detected as a dark amorphous, diaminobenzidine (DAB) reaction product. Note that the PNMT-IR terminal (white T) contains a mixed population of mostly small, clear, pleomorphic vesicles. Some PNMT-IR terminals also contained dense core vesicles. All sections were obtained between cs to + 0.5 mm rostral to the cs.

NIH-PA Author Manuscript
NIH-PA Author Manuscript
NIH-PA Author Manuscript

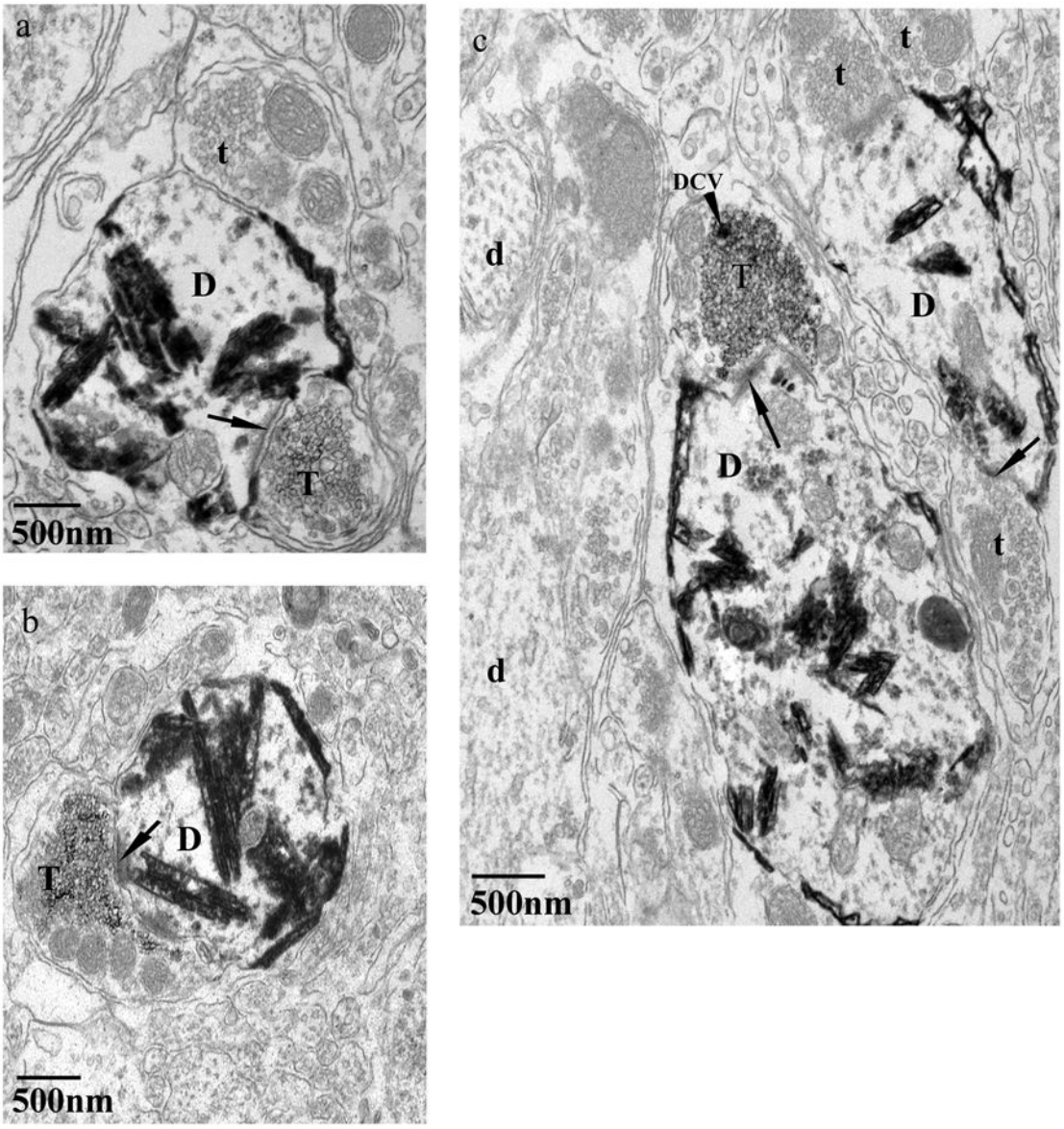

Figure 5.

Axo-dendritic synaptic contacts between dendrites of a fundus-projecting neuron and DβH-IR in the DMV. Figure 5 (a–c): examples of synaptic contact (arrows) between CTβ-HRP-labeled dendrites (D) which were easily identified by dark crystalline TMB-tungstate reaction product, and DβH-IR terminals (T) containing DAB-reaction product. Unlabeled terminals are also identified (t) for comparison. Note that the DβH-IR terminals (T) contain either a mixed population of small, clear, round or pleomorphic vesicles and dense core vesicles (DCV's) (5c) or only small, clear, round or pleomorphic vesicles (5, b). Many synaptic contacts also existed between CTβ-HRP-labeled dendrites and unlabeled terminals (t). An example of an unlabeled terminal forming an apposition with a dendrite of a fundus-projecting neuron is present in 5a.

NIH-PA Author Manuscript
NIH-PA Author Manuscript
NIH-PA Author Manuscript

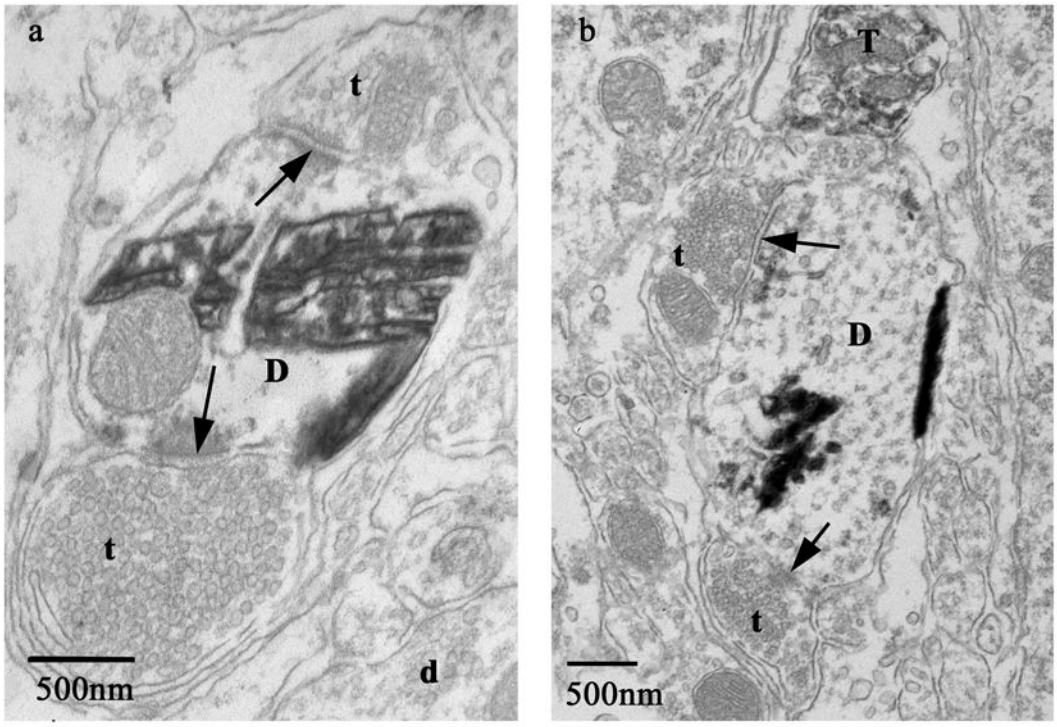

Figure 6.

Axo-dendritic synaptic contacts between dendrites of an antrum-projecting neuron and only unlabeled terminals in the DMV. Figure 6a and 6b: examples of synaptic contact (arrows) between CTβ-HRP-labeled dendrites (D) which were easily identified by dark crystalline TMB-tungstate reaction product, and unlabeled terminals (t). One DβH-IR terminal (T) is also identified (6b) for comparison. Note that the unlabeled terminals (t) contain either a mixed population of small, clear, pleomorphic vesicles and dense core vesicles or only small, clear, pleomorphic or round vesicles (6a, 6b).

NIH-PA Author Manuscript
NIH-PA Author Manuscript
NIH-PA Author Manuscript

Table 1

Summary of the Ultrastructural Analysis of DβH-IR Terminals Forming Synaptic Contacts with DMV Neurons

Area injected with CTβ-HRP	Number of Retrogradely Labeled Profiles Examined	Total Synaptic Contacts with Retrogradely Labeled Profiles	Percent of Synapses Formed with Immunoreactive Terminals	Total Appositions with Retrogradely Labeled Profiles	Percent of Appositions with Immunoreactive Terminals
Fundus	238	476	17.4 +/− 2.7%	400	14.2 +/− 2.2 %
Antrum	223	384	0.0 +/− 0.0%	235	*0.4 +/− 0.4 %

*Only one DβH-IR terminal was found to make an apposition with an antrum-projecting dendrite.

NIH-PA Author Manuscript
NIH-PA Author Manuscript
NIH-PA Author Manuscript

Table 2

Summary of the Ultrastructural Analysis of PNMT-IR Terminals Forming Synaptic Contacts with DMV Neurons

Area injected with CTβ-HRP	Number of Retrogradely Labeled Profiles Examined	Total Synaptic Contacts with Retrogradely Labeled Profiles	Percent of Synapses Formed with Immunoreactive Terminals	Total Appositions with Retrogradely Labeled Profiles	Percent of Appositions with Immunoreactive Terminals
Fundus	165	325	4.4 +/− 0.8%	378	1.2 +/− 1.1%
Antrum	Not done	Not done	Not done	Not done	Not done